MOLECULAR AND CELLULAR BIOLOGY, July 2002, p. 5076–5088 Vol. 22, No. 14
0270-7306/02/$04.00+0 DOI: 10.1128/MCB.22.14.5076–5088.2002

Dissection of a Complex Phenotype by Functional Genomics Reveals Roles for the Yeast Cyclin-Dependent Protein Kinase Pho85 in Stress Adaptation and Cell Integrity

Dongqing Huang, Jason Moffat, and Brenda Andrews*

Department of Medical Genetics and Microbiology, University of Toronto, Toronto, Ontario, Canada M5S 1A8

Received 11 February 2002/Returned for modification 25 March 2002/Accepted 17 April 2002

Cyclin-dependent kinases (Cdks) are key regulators of the cell division cycle. Pho85 is a multifunctional Cdk in budding yeast involved in aspects of metabolism, the cell cycle, cell polarity, and gene expression. Consistent with a broad spectrum of functions, Pho85 associates with a family of 10 cyclins and deletion of *PHO85* causes a pleiotropic phenotype. Discovering the physiological substrates of protein kinases is a major challenge, and we have pursued a number of genomics approaches to reveal the processes regulated by Pho85 and to understand the root cause of reduced cellular fitness in *pho85*Δ mutant strains. We used a functional-genomics approach called synthetic genetic array (SGA) analysis to systematically identify strain backgrounds in which *PHO85* is required for viability. In parallel, we used DNA microarrays to examine the genome-wide transcriptional consequences of deleting *PHO85* or members of the Pho85 cyclin family. Using this pairwise approach coupled with phenotypic tests, we uncovered clear roles for Pho85 in cell integrity and the response to adverse growth conditions. Importantly, our combined approach allowed us to ascribe new aspects of the complex *pho85* phenotype to particular cyclins; our data highlight a cell integrity function for the Pcl1,2 subgroup of Pho85 Cdks that is independent of a role for the Pho80-Pho85 kinase in the response to stress. Using a modification of the SGA technique to screen for suppressors of *pho85*Δ strain growth defects, we found that deletion of putative vacuole protein gene *VTC4* suppressed the sensitivity of the *pho85*Δ strain to elevated $CaCl_2$ and many other stress conditions. Expression of *VTC4* is regulated by Pho4, a transcription factor that is inhibited by the Pho80-Pho85 kinase. Genetic tests and electron microscopy experiments suggest that *VTC4* is a key target of Pho4 and that Pho80-Pho85-mediated regulation of *VTC4* expression is required for proper vacuole function and for yeast cell survival under a variety of suboptimal conditions. The integration of multiple genomics approaches is likely to be a generally useful strategy for extracting functional information from pleiotropic mutant phenotypes.

Cyclin-dependent kinases (Cdks) are heterodimeric protein complexes that are essential activators of cell cycle progression in eukaryotic cells. Cdks promote a variety of cellular events including passage through major cell cycle transitions, initiation of DNA synthesis, entry into anaphase, checkpoint responses, cell state transitions, and precise metabolic controls (2, 46). The regulation of Cdk activity is complex and includes obligate association with positive regulatory subunits called cyclins. Of the five Cdks expressed in budding yeast *Saccharomyces cerevisiae*, two are activated by members of large cyclin families (2, 43, 65). Cdc28 (or Cdk1) is devoted entirely to cell cycle control and is activated by nine cyclins, Cln1 to -3 and Clb1 to -6 (42). Pho85 is the yeast homologue of mammalian CDK5 (23, 50) and, in conjunction with its 10 attendant cyclins or Pcls, has been implicated in a wide variety of cellular processes (12, 45).

Since Pho85 is not essential for viability, it is ideally suited for genetic studies of cyclin-Cdk specificity and function. The 10 Pho85 cyclins can be divided into two subfamilies on the basis of sequence similarity and some genetic and functional information: the Pho80 subfamily (Pho80, Pcl6, Pcl7, Pcl8, and Pcl10) and the Pcl1,2 subfamily (Pcl1, Pcl2, Pcl5, Pcl9, and Clg1) (40). Pho85 was originally identified due to its central role in a signaling pathway that regulates cellular responses to phosphate starvation (reviewed in reference 34). When phosphate is abundant, the Pho80 cyclin directs Pho85 to phosphorylate and inactivate Pho4, a transcription factor required for expression of acid phosphatase genes such as *PHO5* (27, 52). When phosphate is scarce, the Pho80-Pho85 complex is inhibited by CDK inhibitor Pho81, resulting in accumulation of the unphosphorylated and active form of Pho4 in the nucleus (59). *PHO5* and other acid phosphatase (*PHO*) genes are not the only targets of Pho4; expression of a suite of so-called *PHM*/*VTC* genes encoding vacuolar proteins involved in polyphosphate metabolism and vacuole transport is also dependent on Pho4 (51).

More recent studies have identified targets and roles for other forms of Pho85. When Pho85 is activated by one of a pair of closely related cyclins, Pcl8 or Pcl10, it is a potent and specific kinase for Gsy2, an isoform of glycogen synthase (22, 70). Pho85 phosphorylation inhibits glycogen synthase and hence glycogen synthesis and accumulation. The targets of the two remaining Pho80-like cyclins, Pcl6 and Pcl7, remain obscure, although these cyclins have been genetically implicated in glycogen storage, phosphate regulation, and carbon metabolism (32, 68), and expression of *PCL7* peaks during S phase.

Although *PHO85* is not essential, it is required for cell cycle

* Corresponding author. Mailing address: Rm. 4287, Medical Sciences Building, 1 Kings College Circle, Toronto, Ontario, Canada M5S 1A8. Phone: (416) 978-8562. Fax: (416) 971-2494. E-mail: brenda.andrews@utoronto.ca.

progression in the absence of the G_1-specific Cdc28 cyclins, Cln1 and Cln2; this phenotype can be ascribed to the Pcl1 and Pcl2 cyclins, since strains lacking *CLN1*, *CLN2*, *PCL1*, and *PCL2* arrest in G_1 phase of the cell cycle (39). Also, expression of *PCL1*, *PCL2*, and highly related cyclin gene *PCL9* is entirely restricted to G_1 phase of the cell cycle, consistent with roles for these kinases in G_1 phase progression (1, 40, 61). Several observations suggest that the essential function of G_1-specific Pcl-Pho85 complexes relates to cell polarity and morphogenesis. First, deletion of Pcl1,2-type cyclins or Pho85 causes dramatic morphological abnormalities including elongated buds, altered budding pattern, loss of viability and abnormal morphology on starvation, defects in endocytosis, salt sensitivity, and delocalized actin (31). The roster of phenotypes seen in the *pcl*Δ and *pho85*Δ mutants is often seen when the function of actin and actin-associated proteins is compromised. Second, consistent with the phenotypic analysis, an actin-regulatory protein called Rvs167 has been identified as a strong candidate substrate, related to the essential role for Pcl-Pho85 in G_1 phase. Rvs167, the yeast amphiphysin homologue, interacts with Pcl2 and Pcl9 and is phosphorylated in a Pcl1,2-Pho85-dependent manner in vivo (10, 31). However, additional cytoskeletal and morphogenesis targets must also exist; deletion of *RVS167* does not create the same genetic requirements as deletion of *PHO85*, yet tests with mislocalized cyclins clearly show that the essential function of Pcl1,2-Pho85 is cytoplasmic (44). Finally, *PCL1*, *PCL2*, and *PHO85* show genetic interactions with genes known to be involved in cell morphogenesis and polarity (33). Together, these data establish a role for G_1-specific Pho85 kinases in cell morphogenesis and polarity, but precise functions and additional targets remain to be discovered.

Pho85 has also been implicated in promoting the instability and degradation of several proteins: (i) Sic1, a Cdk inhibitor that restrains S phase (49); (ii) Gcn4, a transcription factor required for increased expression of amino acid-biosynthetic genes upon amino acid starvation (8, 41); (iii) Swi5, a transcription factor required for cell cycle-dependent expression of a variety of genes (38); and (iv) Ash1, a daughter cell-specific transcriptional repressor (37). In addition, conventional and chemical genetics experiments have suggested roles for Pho85 in autophagy (69), proline utilization (55), and environmental stress response (5). As highlighted above, certain *pho85* phenotypes can be reproduced by deletion of cyclins, but, for the most part, we lack a comprehensive understanding of cyclin function and relevant biological substrates for the various Pho85 Cdks.

In this study, we married phenotypic tests with functional-genomics approaches including transcriptional profiling and systematic genetic arrays to explore Pho85 and Pcl function. We reasoned that Pho85 function should be reflected in both the global transcription pattern and the genetic interaction network of *pho85*Δ and *pcl*Δ mutants. Our systematic genomics approaches have revealed novel roles for Pho85 Cdks in stress adaptation and cell wall integrity.

MATERIALS AND METHODS

Strains and media. *S. cerevisiae* strains used in this study are listed in Table 1. Standard methods and media were used for yeast growth and transformation (20). Standard rich medium with glucose (yeast extract-peptone-dextrose [YPD] medium) was supplemented with NaCl, $CaCl_2$, sorbitol, and different drugs to create stress conditions. Supplemented minimal medium (synthetic dextrose [SD]) with appropriate amino acid supplements was used for maintaining plasmids in yeast transformants and for genetic selection (20). All gene disruptions were achieved by homologous recombination at their chromosomal loci by standard PCR-based methods (35).

TABLE 1. *S. cerevisiae* strains used in this study[a]

Strain(s)	Genotype	Reference or source
BY263	*MAT***a** *trp1 leu2 his3 ura3 lys2 ade2*	39
BY391	*MAT***a** *pho85ΔLEU2*	39
BY490	*MAT***a** *pho80ΔHIS3*	40
BY714	*MAT***a** *pcl1ΔLEU2 pcl2ΔLYS2 pcl5ΔTRP1 clg1ΔURA3 pcl9ΔHIS3*	40
BY1500	*MAT***a** *pho80ΔHIS3 pho4ΔTRP1*	This study
BY1501	*MAT***a** *pho80ΔHIS3 vtc4ΔTRP1*	This study
BY1530	*MAT***a** *pho85ΔLEU2 pho4ΔTRP1*	This study
BY1534	*MAT***a** *pho85ΔLEU2 vtc4ΔTRP1*	This study
Y4742	*MATα ura3Δ3 leu2Δ0 his3Δ1 lys2Δ0 met15Δ0*	71
Consortium strains	*MAT***a** *ura3Δ3 leu2Δ0 his3Δ1 met15Δ0 xxx::KAN*^{r}	71
Y2454	*MATα mfa1::MFA1pr-HIS3 can1Δ ura3Δ0 leu2Δ0 his3Δ1 lys2Δ0 MET15*$^+$	64
BY1502	Y2454 *MATα pho85ΔLEU2*	This study

[a] Strains are isogenic to the parent BY263 unless indicated. Y4742 is the parent strain for the yeast deletion consortium strains (71), which are also of S288C origin. Y2454 is isogenic to Y4742, and BY1502 is a derivative of Y2454 carrying a *pho85ΔLEU2* disruption allele.

DNA microarray analysis. Yeast strains were grown in rich medium at 30°C to an optical density at 600 nm (OD_{600}) of 0.5. Cells were harvested by centrifugation and then quickly frozen in liquid nitrogen. Cell pellets were stored at −80°C until RNA was prepared. Total RNA and poly(A)$^+$ RNA were isolated as previously described (3). DNA microarrays with >97% genome coverage were probed with differentially labeled cDNA pools from wild-type and mutant strains essentially as described at http://www.oci.utoronto/ca/microarrays. Arrays were obtained from the Ontario Cancer Institute Microarray facility (see the website above), and differential labeling of cDNA was achieved with Cy3-dCTP or Cy5-dCTP (Mandel). The hybridized arrays were scanned with a Gene Pix 4000B scanner (Axon Instruments). The expression ratios of open reading frames (ORFs) between mutant and wild-type cells were calculated by using intensities adjusted to medians. Artifacts were removed from the data set after visually inspecting the spots. The expression profile of the *pho85*Δ mutant used in the fingerprint match was an average of six independent experiments. Other profiles used were averages of two experiments.

Expression ratios of yeast ORFs from experiments with *pho85*Δ and *pcl* strains were aligned with corresponding ratios from 300 experiments published by Rosetta Inpharmatics (24). Simple Pearson correlation coefficients (ρ) were calculated by using a Microsoft Excel function. The calculation used either expression data for all ORFs in the genome or those for 546 genes selected by Rosetta as representative of genes involved in various regulatory pathways (24). Calculations using both sets of data gave similar results.

Systematic synthetic-lethal screen. We used the synthetic genetic array (SGA) method to systematically identify mutant backgrounds in which *PHO85* is required for viability (64). First, a 20-ml culture of strain BY1502 was grown overnight in YPD. The culture was then pinned on YPD agar medium prepared in Omni trays with multiblot floating pin replicators and a VP380 colony copier guide (V&P Scientific). Arrays of the yeast deletion consortium strains from a series of Omni plates were then pinned on top of the BY1502 strain array. The mating reaction was allowed to proceed overnight at 30°C, and diploids were then selected by pinning cells onto SD plates lacking Leu and Lys. To sporulate the diploids, the cells were pinned onto sporulation plates and incubated at room temperature for 7 days. The spores were then pinned onto SD plates lacking His, Leu, and Arg and containing canavanine (70 μg/ml) to select *MAT***a** *pho85ΔLEU2* haploid cells (64). The haploid selection was repeated twice by repinning to fresh selective medium. Finally, to select double mutants, the *MAT***a** *pho85ΔLEU2* cells were pinned and resuspended in 200 μl of sterilized water in 96-well plates. The suspension of cells was then pinned onto YPD–G-418 (200 μg/ml) plates and incubated at 30°C for 2 days. This dilution step significantly reduced the number of cells transferred to fresh media on a single pinhead and

aided in selection against spontaneous suppressors that arise in the slowly growing *pho85*Δ strain. *spt7*, *srb5*, and *hfi1* single mutants were not recovered in this screen from sporulation of diploids created by crossing these mutants to the wild type; therefore, we cannot score these mutants in our *pho85*Δ screen. Synthetic lethality was scored as described previously (64) at the positions where double-mutant colonies failed to grow.

In a second screen, consortium strains were crossed to BY1502 harboring a *URA3*-based plasmid (pRS316 backbone) and a wild-type *PHO85* gene expressed from its own promoter (pBA1468). The double mutants were selected essentially as described for the primary screen except that uracil was removed from the selective medium to maintain the p*PHO85* plasmid. We first eliminated mutants that scored as synthetically lethal with BY1502(pPHO85) (note that 527 mutants including the *spt7, hfi1*, *srb5*, and *srb10*/*11* mutants were eliminated at this step; see above). The remaining strains were pinned onto 5-fluoroorotic acid (5-FOA) plates. Double mutants that showed sensitivity to 5-FOA (that is, dependence on p*PHO85* for viability) were picked for colony purification (255 strains passed this test). Single colonies were patched onto fresh medium and tested again for sensitivity to 5-FOA; confirmed 5-FOA-sensitive colonies were selected for further confirmation by random spore analysis (97 strains). Briefly, the original deletion strains carrying the candidate gene disruptions were crossed to BY1502 again. The selection of diploids, sporulation, and the selection of *MAT***a** *pho85*Δ*LEU2* haploid cells after sporulation were essentially the same as in the primary screen. These *MAT***a** *pho85*Δ*LEU2* haploid cells were then restreaked onto fresh medium, and 36 single colonies were checked for the existence of double mutants (Leu^+ and G-418 resistance). If no double mutants were recovered from the progeny spores, strains with the original gene deletions were defined as true positives.

Zymolyase sensitivity assay. Spheroplast lysis was measured by following published procedures (53). BY263, BY391, BY490, and BY714 cultures were grown to log phase (OD_{600} = ~0.5) in YPD at 30°C. Cells were harvested, washed, and resuspended in 1 ml of Tris-EDTA (pH 8.2) so that the final OD_{600} was about 0.5. Three microliters of Zymolyase 100T (1 mg/ml) was then added. The OD_{600} of the cultures was checked every 5 min for each sample. Lag time, the maximal lysis rate, and the rate index were calculated as described previously (53).

Fluorescence microscopy. FM4-64 [*N*-(3-triethylammoniumpropyl)-4-(*p*-diethylaminophenylhexatrienyl) pyridinium dibromide; Molecular Probes] and Lucifer yellow (LY; Sigma) staining was carried out as described previously (20, 67). Briefly, cultures were grown to mid-log phase in YPD and either FM4-64 or LY was added. FM4-64 staining was allowed to proceed for 15 min. The cultures were then washed, and FM4-64 accumulation was visualized with rhodamine fluorescence optics at a magnification of ×1,000. Cells were stained with LY for 30 to 60 min, washed four or five times in phosphate-buffered saline, and viewed through a fluorescein isothiocyanate filter to observe LY fluorescence. Photographs were taken with a Micromax 1300y high-speed digital camera (Princeton Instruments, Trenton, N.J.) mounted on a Leica DM-LB microscope. Images from the camera were analyzed with Metaview software (Universal Imaging, Media, Pa.).

Electron microscopy. Strains were grown in YPD at 30°C to mid-log phase, centrifuged, washed in H_2O, and prepared for electron microscopy by procedures modified from those described by Friesen et al. (16). In brief, cells were fixed for 3 h in aldehyde fixative (3% acrolein, 2.5% glutaraldehyde, 0.1 M sodium cacodylate, pH 6.5) at room temperature and then overnight at 4°C. Fixative was removed and replaced with fresh aldehyde fixative for an additional 24 h at 4°C. Samples were washed and postfixed in 1.5% potassium permanganate for 30 min in the dark at room temperature, washed again, and fixed with 1% osmium tetroxide in cacodylate buffer for 1 h in the dark at room temperature. Dehydration was performed by using a graded series of ethanol steps. The cell pellets were infiltrated with Spurr's epoxy resin by using a graded series of mixtures of Spurr's resin and ethanol. The final infiltration with 100% Spurr's resin proceeded for 72 h to ensure that all of the yeast cells were completely infiltrated. Thin sections were stained with uranyl acetate for 15 min followed by Reynold's lead citrate for 15 min and examined on a Hitachi H7000 transmission electron microscope at an accelerating voltage of 75 kV.

Second-site suppressor screen. The *pho85*Δ double mutants generated from the synthetic-lethal screen (see above) were first pinned and resuspended in 200 μl of sterilized water in 96-well plates. The suspension of cells was then pinned onto YPD plates supplemented with either 6% NaCl, 10 ng of rapamycin/ml, or 200 mM $CaCl_2$. After incubation at 30°C (2 days for plates with $CaCl_2$, 4 days for plates with NaCl or rapamycin), the positions with colony growth were scored and primary candidate suppressor genes were identified according to their positions.

Only the calcium suppressor screen gave promising preliminary results, and the primary candidate suppressor strains were crossed to BY1502. The selection of diploids, sporulation, and the selection of *MAT***a** *pho85*Δ*LEU2* haploid cells after sporulation were essentially the same as described above for the synthetic-lethal screen. The haploid cells were then streaked for single colonies on fresh medium; in this case, both the *pho85*Δ*LEU2* single mutant and *pho85*Δ*LEU2* *xxx*::*KAN*^{r} double mutants were present in the cell population. Thirty-six single colonies were picked and were tested for growth on YPD-$CaCl_2$ (200 mM) and YPD–G-418 (200 μg/ml). If G-418-resistant colonies were able to grow on YPD-$CaCl_2$ (200 mM) and if colonies able to grow on YPD-$CaCl_2$ were G-418 resistant, strains with the original gene deletions were defined as true positives.

RESULTS

Identification of genes required for viability in the absence of *PHO85* using SGA analysis. To explore the processes regulated by *PHO85*, we took advantage of a recently developed method to systematically construct double mutants in the *pho85*Δ background by crossing to an ordered array of viable gene deletion mutants (64). Briefly, a *pho85*Δ strain was crossed to an array of approximately 4,200 deletion strains (64, 71) by a replica pinning procedure. The resulting diploids were selected and sporulated, and haploid double mutants carrying both the *pho85*Δ allele and a second gene disruption were selected by using the markers in the starting strain (64). Double-mutant strains that failed to grow defined candidate genetic backgrounds in which *PHO85* was required for viability. After eliminating false positives that also showed a synthetic-lethal interaction with the *pho85*Δ strain harboring *PHO85* on a plasmid (see Materials and Methods), 53 yeast gene disruptions were confirmed by random spore analysis to cause synthetic lethality in a *pho85*Δ strain.

Genes that required *PHO85* for viability were organized into seven categories according to their roles as defined by the Yeast Proteome Database (Fig. 1) (www.proteome.com.). The first category defines 32% of the *pho85*Δ synthetic-lethal interactions and includes genes required for cell wall maintenance and/or integrity. This category can be further subdivided into genes that encode machinery for cell wall construction and those that are part of or have been implicated in the cell integrity signaling cascade (19). The cell wall genes include (i) *ANP1*, *MNN10*, and *HOC1*, which encode components of the Anp1-Hoc1-Mnn9-Mnn10-Mnn11 mannosyltransferase complex of the Golgi (26); (ii) *VAN1*, which encodes a component of the mannan polymerase complex (26); (iii) *FKS1*, which provides an essential function that overlaps with that of *GSC2* in the construction of cell wall glucan (60); (iv) *FKS3*, which encodes a protein with similarity to those encoded by *FKS1* and *GSC2*; (v) *SHC1*, which encodes a protein involved in cell wall chitin synthesis and deposition; and (vi) *PMR1* and *ERD1*, which are both required for glycosylation of cell wall proteins (21, 58). This profile of genetic interactions suggests that *pho85*Δ cells must maintain the ability to glycosylate proteins and lay down cell wall glucan in order to survive.

The second subset of genes in the first category includes genes in the so-called cell integrity signaling cascade. *WSC1*/*HCS77*/*SLG1* and *WSC4* encode similar membrane proteins, which may act as cell integrity sensors (66), while *ROM2* encodes an exchange factor for the Rho1 GTPase that is required for signaling into the protein kinase C–Slt2 mitogen-activated protein kinase (MAPK) cell integrity cascade (11). *BCK1* and *SLT2*/*MPK1* encode nonredundant MAPK kinase kinase and MAPK, respectively, in the cell integrity MAPK pathway (19).

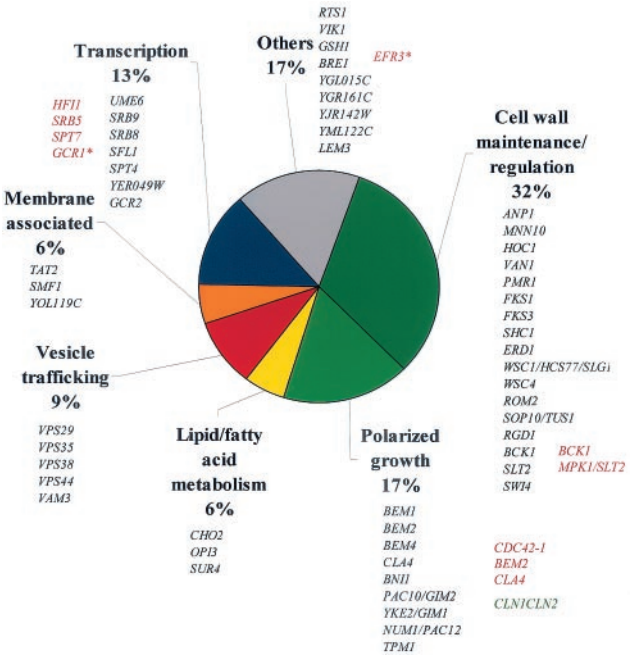

FIG. 1. Pie chart summarizing the results of the *pho85*Δ SGA synthetic-lethal screen. Genes were categorized according to their annotations in the Yeast Proteome Database (www.proteome.com). Genes in red were discovered as "85-requiring" genes by Lenburg and O'Shea (34). Synthetic lethality of the *pho85 cln1 cln2* strain was previously reported (14, 33, 39).

SWI4 encodes the DNA-binding component of G_1 cell cycle transcription factor complex SBF, which is a downstream target of the Slt2-MAPK pathway (36). *SOP10*/*TUS1* and *RGD1* encode signaling molecules that may also be involved in the cell integrity cascade. These results establish that the cell integrity pathway is indispensable in the absence of *PHO85*.

The second major category, which overlaps functionally with the cell integrity group, defines 17% of the *pho85*Δ synthetic-lethal interactions and includes genes required for polarized growth and spatial regulation (Fig. 1). *BEM1*, *BEM2*, *BEM4*, and *CLA4* encode proteins required for proper bud emergence and polarity establishment (25). *BEM1* encodes an SH3 and PX domain-containing protein that interacts with cell polarity GTPase Cdc42 and its activator Cdc24 (13). *BEM2* encodes a GTPase-activating protein for Rho-type GTPases, and *BEM4* encodes a protein that interacts with Rho-type GTPases and that is linked to Rho1-Pkc1 signaling. *CLA4* encodes a mammalian PAK-like protein kinase, and *BNI1* encodes a yeast formin; both of these proteins are effectors of Cdc42 function (56). These results indicate the importance of spatial regulation in the absence of *PHO85*.

The remaining genes that create a genetic requirement for *PHO85* have roles in transcription (*UME6*, *SRB9*, *SRB8*, *SFL1*, *SPT4*, *YER049W*, and *GCR2*), lipid and/or fatty acid metabolism (*CHO2*, *OPI3*, and *SUR4*), and vesicle trafficking (*VPS29*, *VPS35*, *VPS38*, *VPS44*, and *VAM3*). There are also several genes that encode membrane-associated proteins (*TAT2*, *SMF1*, and *YOL119C*) and a large group of genes that have not been ascribed to a particular category or whose function remains unknown (Fig. 1).

Expression profiling of *pho85*Δ and *pcl*Δ strains reveals a novel signature related to cell wall and ergosterol mutants. In a parallel approach to identify functions for Pho85 kinases, we examined the genome-wide transcriptional consequences of deleting *PHO85* or one or multiple members of the Pho85 cyclin family. As expected, we observed obvious up-regulation of Pho4-dependent genes, including *PHO* and *PHM*/*VTC* genes in the absence of *PHO85* or *PHO80* (Fig. 2A) (5, 51). Other changes in *pho85*Δ cells relative to the wild type included increased expression of some stationary-phase and amino acid biosynthesis genes and decreased expression of translation-related genes (data not shown; full data set available at http://www.utoronto.ca/andrewslab). To extract functional information from the *pho85*Δ and *pcl*Δ profiles, we compared our microarray data from 19 *pho85*Δ- or *pcl*Δ-related strains to an array of published experiments available on the World Wide Web using the compendium approach first described by Hughes et al. (24) (Fig. 2B). An arbitrary ρ of >0.2 was determined to be significant following 10 randomization trials of the *pho85*Δ strain data that gave an average ρ (ρ_{avg}) ± standard error of 0.0060 ± 0.0088 (Fig. 2B). Comparison of the data to a compendium of expression profiles using ρ revealed a *pho85*Δ signature profile that showed significant similarity ($\rho > 0.4$) to those of mutants with defects in either cell wall or ergosterol biosynthesis, regardless of whether the expression ratios from all ~6,000 genes in yeast or a group of 546 representative genes were used to calculate ρ. The 10 mutant signatures that were most closely correlated to the *pho85*Δ profile were further compared to *pho85*Δ *pho4*Δ, *pho80*Δ, and quintuple (*pc1*Δ *pcl2*Δ *pcl5*Δ *pcl9*Δ *clg1*Δ) signatures to determine whether the *pho85*Δ correlation results were due to the transcription factor Pho4, the Pcl1,2 subfamily of cyclins, or the Pho80 cyclin (Fig. 2C). Interestingly, the *pho85*Δ *pho4*Δ, quintuple, and *pho80*Δ strain profiles all correlated positively with the same top 10 strains in our *pho85*Δ comparison but to a significantly lesser degree (Fig. 2C). Although deletion of *PHO4* in a *pho85*Δ background results in a reduced degree of correlation to the top 10 mutants, these results also indicate that the *pho85*Δ expression signature is not attributable to a distinct cyclin or subfamily of cyclins. In summary, the *pho85*Δ expression profile suggests that *PHO85* may have a broad role in cell integrity and/or ergosterol biosynthesis and corroborates the SGA profile, pointing to a role for *PHO85* in cell integrity.

A *pho85*Δ strain does not have ergosterol defects. The presence of two ergosterol mutants (*erg2*Δ and *erg6*Δ mutants) was among the top 10 conditions that positively correlated with the *pho85*Δ expression profile (Fig. 2C). Ergosterol is a major component of the yeast cell membrane and is required for normal membrane dynamics (54). Since the *pho85*Δ expression profile suggested that *PHO85* may be related to ergosterol function, we assayed the sensitivity of *pho85*Δ cells to specific drugs. Miconazole inhibits ergosterol biosythesis, and nystatin binds ergosterol to exert its toxic effects (17). Thus, mutants with defects in ergosterol biosynthesis are sensitive to miconazole and resistant to nystatin. A plating assay revealed that *pho85*Δ cells were insensitive to miconazole (0.05 μg/ml) and mildly sensitive to nystatin (data not shown). Subsequent biochemical analysis of major sterols failed to show any significant differences between *pho85*Δ and wild-type cells (Martin Bard, Purdue University, personal communication), indicating that

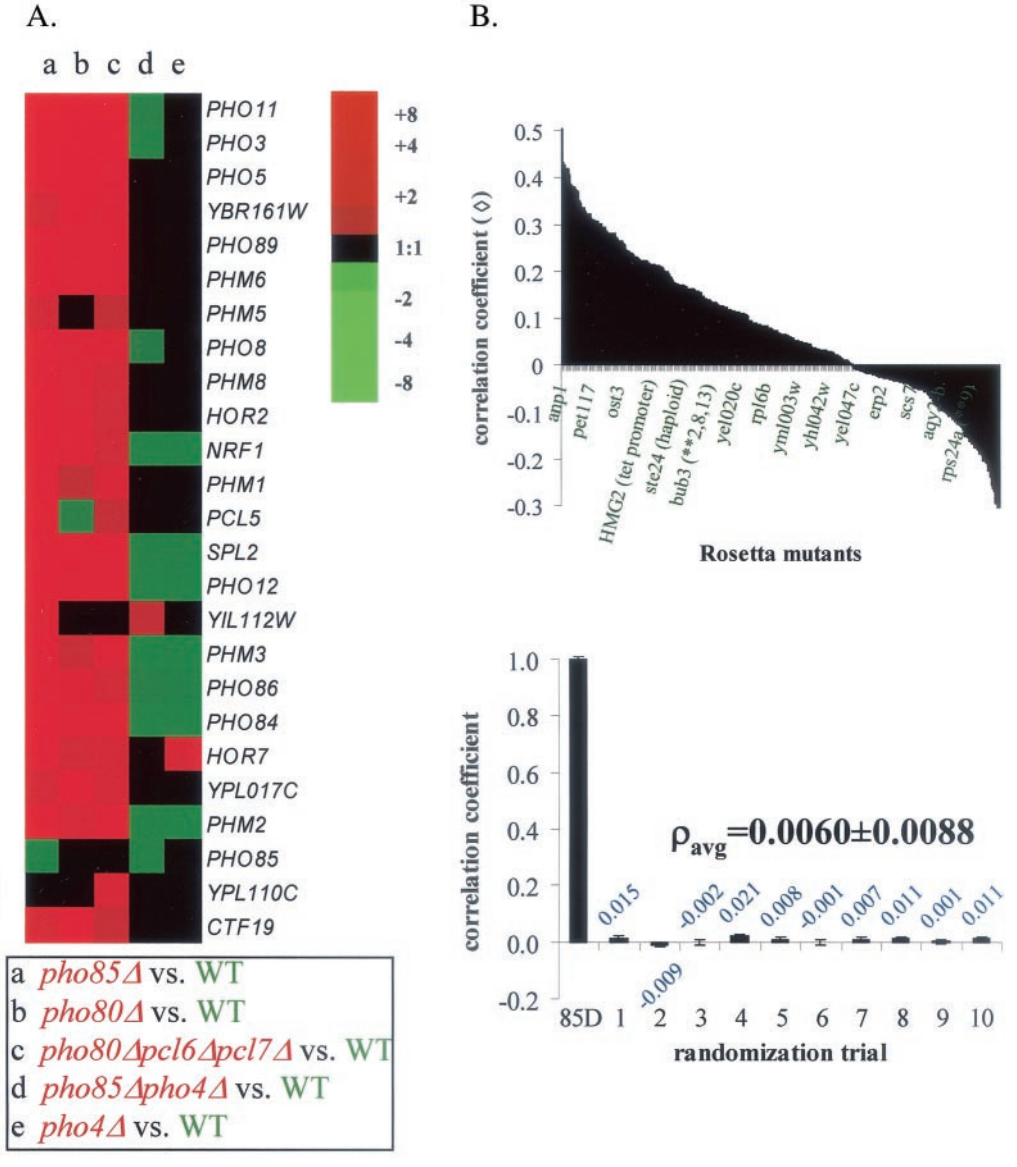

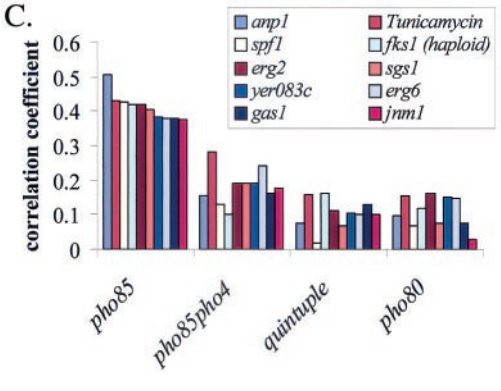

FIG. 2. Expression profiling of yeast strains lacking *PHO85* or one or multiple members of the Pho85 cyclin family genes. (A) Expression ratio analysis of *pho85*Δ and related strains showing the archetypal *PHO* cluster. The cluster was generated with AFM4.0 Toolbox, available on the World Wide Web. The color ratio scale is shown to the right. The experiment list is shown below the cluster. WT, wild type. (B) (Top) Comparison of the expression signature of the *pho85*Δ (BY391) strain with a database of expression profiles for 546 representative genes published by Hughes et al. (24). Values of ρ for the expression signature of *pho85*Δ cells against 300 Rosetta mutant profiles are plotted. (Bottom) *pho85*Δ expression ratios were randomized and correlated to the original *pho85*Δ ratios. The histogram shows the control (85D; ρ = 1.0) and 10 randomization trials. The average ρ for 10 randomization trials (ρ_{avg}) was 0.0060 ± 0.0088, validating the significance of a ρ of >0.1. (C) Histograms representing the top 10 Rosetta mutants whose profiles correlate to the *pho85*Δ expression signature and comparison with *pho85*Δ *pho4*Δ, quintuple-mutant (*pcl1*Δ *pcl2*Δ *pcl5*Δ *pcl9*Δ *clg1*Δ), and *pho80*Δ strain expression signatures using expression ratios from 546 representative genes. Some Rosetta mutants are indicated.

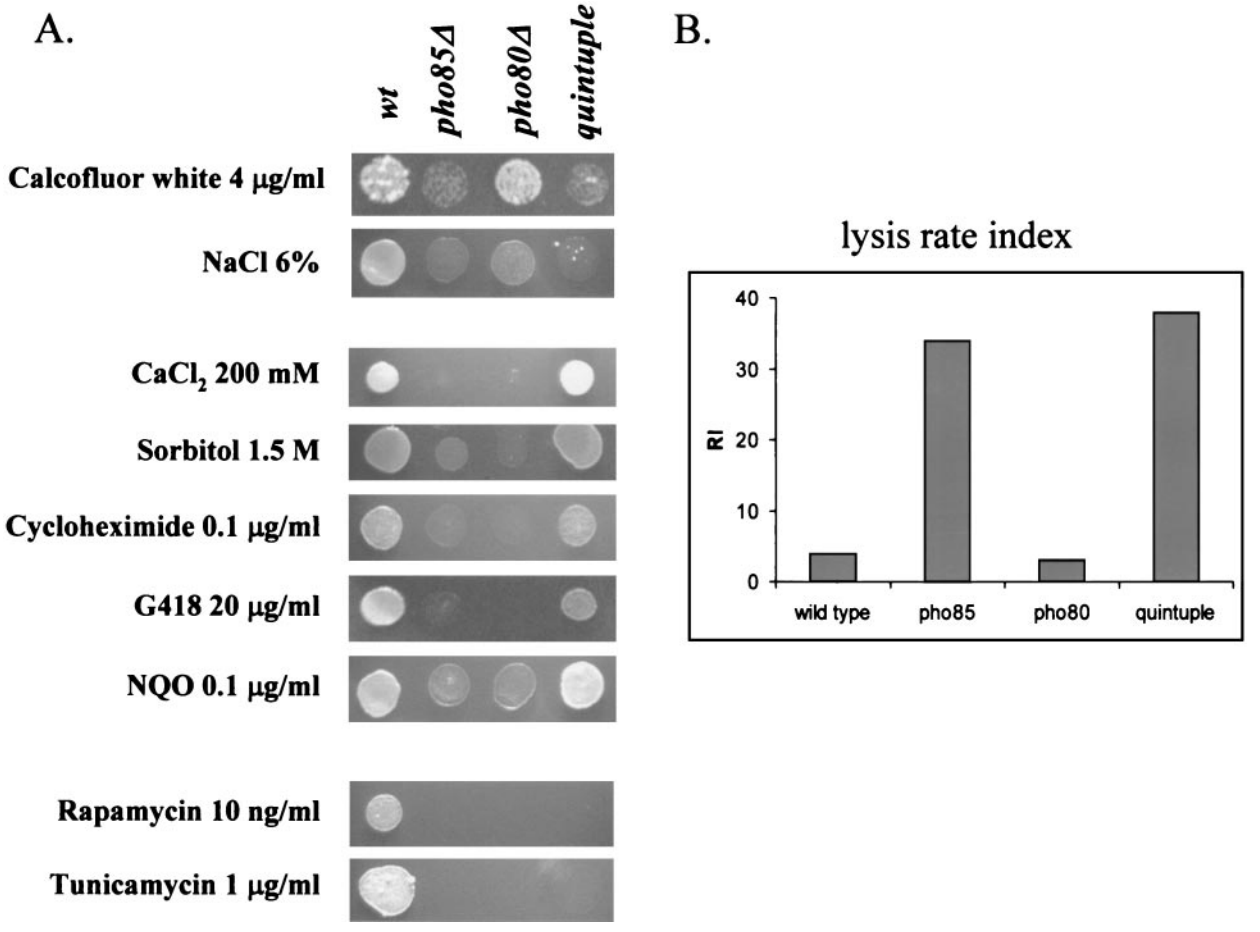

FIG. 3. Cell integrity and stress sensitivity phenotypes of wild-type, *pho85*Δ, *pho80*Δ, and quintuple-mutant strains. (A) Effects of stress conditions on the growth of wild-type (*wt*; BY263), *pho85*Δ (BY391), *pho80*Δ (BY490), and quintuple-mutant (BY714; *pcl1*Δ *pcl2*Δ *pcl5*Δ *pcl9*Δ *clg1*Δ) strains. Approximately 10^4 cells in mid-log phase were spotted onto YPD containing either calcofluor white, NaCl, sorbitol, $CaCl_2$, 4-NQO, cycloheximide, G-418, rapamycin, or tunicamycin at the indicated concentrations. Plates were incubated for 2 to 7 days at 30°C and photographed. (B) Spheroplast lysis rates for wild-type (BY263), *pho85*Δ (BY391), *pho80*Δ (BY490), and quintuple-mutant (BY714; *pcl1*Δ *pcl2*Δ *pcl5*Δ *pcl9*Δ *clg1*Δ) strains. RI, rate index (see Materials and Methods). One of three representative experiments is shown.

the biosynthesis of sterol components is intact in *pho85*Δ cells. We conclude that the cell integrity defects in *pho85*Δ cells are not related to ergosterol biosynthesis or function.

Phenotypic assays reveal broad sensitivity to cell stressors and cell integrity insults in cells lacking Pho85 kinases. Our functional genomics screens suggest a major problem with cell integrity in *pho85*Δ cells. To begin to explore the basis of this complex phenotype, we assayed the growth of wild-type and *pho85*Δ strains under several conditions that affect cell integrity. We included *pho80*Δ and quintuple (*pc1*Δ *pcl2*Δ *pcl5*Δ *pcl9*Δ *clg1*Δ) mutant strains in these sensitivity assays to observe phenotypes that may be ascribed to particular Pho85 cyclins. The remaining members of the Pho80 subfamily, Pcl6, Pcl7, Pcl8, and Pcl10, did not factor into the sensitivity assays (data not shown). Two compounds commonly used to test cell wall integrity are calcofluor white and tunicamycin; calcofluor white interferes with cell wall biosynthesis and is used to track cell wall biosynthesis mutants, while tunicamycin specifically inhibits the product of the *ALG7* gene, which is required for protein N glycosylation (57, 60). Both the *pho85*Δ mutant and the quintuple-mutant strain failed to grow in the presence of either calcofluor white or tunicamycin (Fig. 3A). Consistent with our genome-wide phenotypic scans, these results show that *pho85*Δ cells are sensitive to agents that compromise the integrity of the cell.

Many strains with cell integrity defects show sensitivity to a broad range of stressors; indeed, *PHO85* has been shown to be indispensable in cells exposed to stresses such as growth on nonfermentable carbon sources or in the presence of high salt (31, 63). To further probe the cell integrity status of *pho85*Δ mutants, we expanded our phenotypic survey to include a broad range of conditions. We selected conditions that either enhance or impair the growth of known cell integrity mutants, such as high osmolarity or salt, as well as several unrelated conditions. *pho85*Δ cells were found to be markedly sensitive to high levels of osmolarity (1.5 M sorbitol), salt (6% NaCl or 1 M KCl), Ca^{2+} (200 mM $CaCl_2$), the immunosuppressant rapamycin, the DNA-damaging reagent 4-NQO (4-nitroquinoline *N*-oxide), and protein synthesis inhibitors cycloheximide and Geneticin (Fig. 3A). Since both the quintuple and *pho85*Δ mutants have defects in cell wall integrity, we were surprised to find that the quintuple mutant was only sensitive to high salt

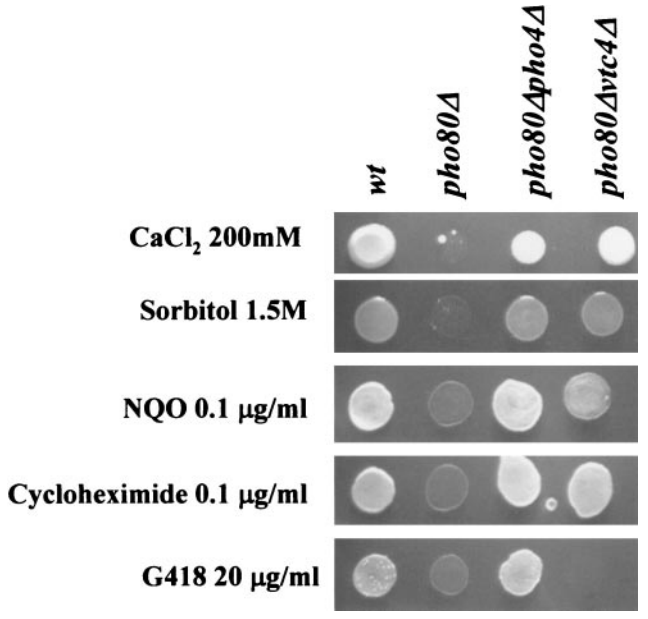

FIG. 4. Rescue of several *pho80*Δ phenotypes by deletion of *PHO4* or *VTC4*/*PHM3*. Growth of wild-type (*wt*), *pho80*Δ, *pho80*Δ *pho4*Δ, and *pho80*Δ *vtc4*Δ strains on medium containing various compounds is shown. Approximately 10^4 cells in mid-log phase were spotted onto YPD plates containing either $CaCl_2$, sorbitol, 4-NQO, cycloheximide, or G-418 at the concentrations indicated. Plates were incubated at 30°C for 3 days and photographed.

and rapamycin, in addition to calcofluor white and tunicamycin. In contrast, the *pho80*Δ mutant showed a broader profile of sensitivities, which more closely resembled that for the *pho85*Δ phenotype mutant (Fig. 3A). Importantly, only rapamycin and tunicamycin sensitivity was seen in both the *pho80* and quintuple-mutant strains, suggesting that different Pho85 complexes must account for distinct aspects of the stress sensitivity phenotype of the *pho85* mutant.

Yeast cells that have integrity defects have an increased lysis rate following cell wall digestion (53). Therefore, we next used a spheroplast lysis rate index to directly assess the integrity of *pho85*Δ, *pho80*Δ, and quintuple-mutant cells. In this assay, both the *pho85*Δ and quintuple-mutant strains had elevated lysis rate indices relative to wild-type cells (Fig. 3B; six- to sevenfold increase over wild type). By contrast, the *pho80*Δ strain had a lysis rate index comparable to that of the wild type (Fig. 3B). These results clearly show that the integrity defect in *pho85*Δ cells is due to the Pcl1,2 subfamily of cyclins. We infer that the broad sensitivity of *pho80*Δ mutants to a variety of insults must reflect a distinct defect.

Several observations suggest that the sensitivity profile of the *pho80*Δ mutant may be due to a role for Pho80-Pho85 in vacuolar integrity or function. The vacuole is required for detoxification of harmful compounds, autophagy, pH balance, osmobalance, and a number of other functions, all of which coordinate to maintain cellular homeostasis (4). First, *pho85*Δ and *pho80*Δ cells are sensitive to calcium ions and cannot grow on nonfermentable carbon sources, phenotypes seen in mutants with defects in vacuolar function (Fig. 3A and 4 and data not shown) (15, 18, 29). Second, Pho80 is required for proper vacuolar inheritance (47, 48), and five of the *pho85*Δ synthetic-lethal interactions identified in our SGA screen involve genes with roles in vacuolar protein sorting (*VPS29*, *VPS35*, *VPS38*, and *VPS44*) or vacuolar morphology (*VAM3*) (Fig. 1). We used lipophilic dye FM4-64 to monitor bulk membrane internalization and transport to the vacuole in wild-type, *pho80*Δ, *pho85*Δ, and quintuple-mutant cells. After 15 min of staining, FM4-64 was clearly visible on the vacuolar membranes of wild-type and quintuple-mutant cells (Fig. 5). FM4-64 staining of wild-type yeast cells reveals multilobed vacuoles with uniform staining around the vacuolar membranes (67). By contrast, *pho80*Δ and *pho85*Δ mutants showed enlarged vacuoles with abnormal accumulations of fluorescence either on the vacuolar membrane in *pho80*Δ cells or in the cytoplasm in *pho85*Δ cells (Fig. 5). Fluorescent spots in the cytoplasm of *pho85*Δ cells may represent trapped vesicles (67). These results clearly show that *pho80*Δ and *pho85*Δ cells have defects in bulk membrane internalization to the vacuole. Taken together, these experiments corroborate our genomics screens and reveal a significant cell integrity defect in *pho85*Δ mutants that can be largely attributed to the Pcl1,2 subfamily of cyclins and a potential vacuole-related defect in *pho85*Δ mutants that can be ascribed to the Pho80 cyclin.

An SGA suppressor screen reveals a requirement for the Pho4 target *VTC4*/*PHM3* for *pho85*Δ- and *pho80*Δ-related stress phenotypes. So far, our functional genomics approaches and phenotypic assays suggest a role for Pho85 in cell integrity; attempts to assign specific cyclins to aspects of the cell integrity function of Pho85 point to a role for Pho80 in stress response that may be separate from the functions of other Pcls in maintaining cell integrity. In an effort to further delineate aspects of the cell stress and integrity functions of Pho85 and its cyclins, we made use of the genetic array of *pho85*Δ *xxx*Δ double-mutant strains created during the course of the SGA synthetic-lethal screen (Fig. 6). We reasoned that we could systematically screen for deletion mutants (genomic suppressors) that rescue *pho85*Δ phenotypes by printing the genetic array of *pho85*Δ *xxx*Δ double-mutant strains to selected media and screening for survivors (7). Our modification of the SGA method to identify genetic suppressors demands a highly penetrant initial phenotype; we chose 6% NaCl, 200 mM $CaCl_2$, and 10 ng of rapamycin/ml as our screening conditions (Fig. 6). We also chose these conditions since they represent a *pho85* mutant phenotype that is specific to the Pcl1,2-type cyclins (NaCl), the Pho80 cyclin ($CaCl_2$), or both (rapamycin) (Fig. 3A). Briefly, the *pho85*Δ *xxx*Δ double mutants were printed on YPD plates containing either NaCl, $CaCl_2$, or rapamycin and incubated at 30°C. Gene disruptions that suppressed the *pho85*Δ strain sensitivities were scored by observing obvious growth and then identified according to their positions on the array (see Materials and Methods). No suppressors of *pho85*Δ cells in high salt were found, and only deletion of *FPR1*, which encodes the rapamycin-binding protein in yeast, allowed for growth in the presence of 10 ng of rapamycin/ml. However, our screen for *pho85*Δ cell suppressors in Ca^{2+} yielded six positives, including genes involved in osmoregulation (*SKN7*, *SHO1*, *SSK1*, and *SSK2*) (19), the cyclic AMP pathway (*PDE2*) (62), and regulation of vacuolar function (*VTC4*/*PHM3*). We have not pursued the basis of the suppression by the osmoregulators or *PDE2*. Rather, we chose to focus on *VTC4*, since

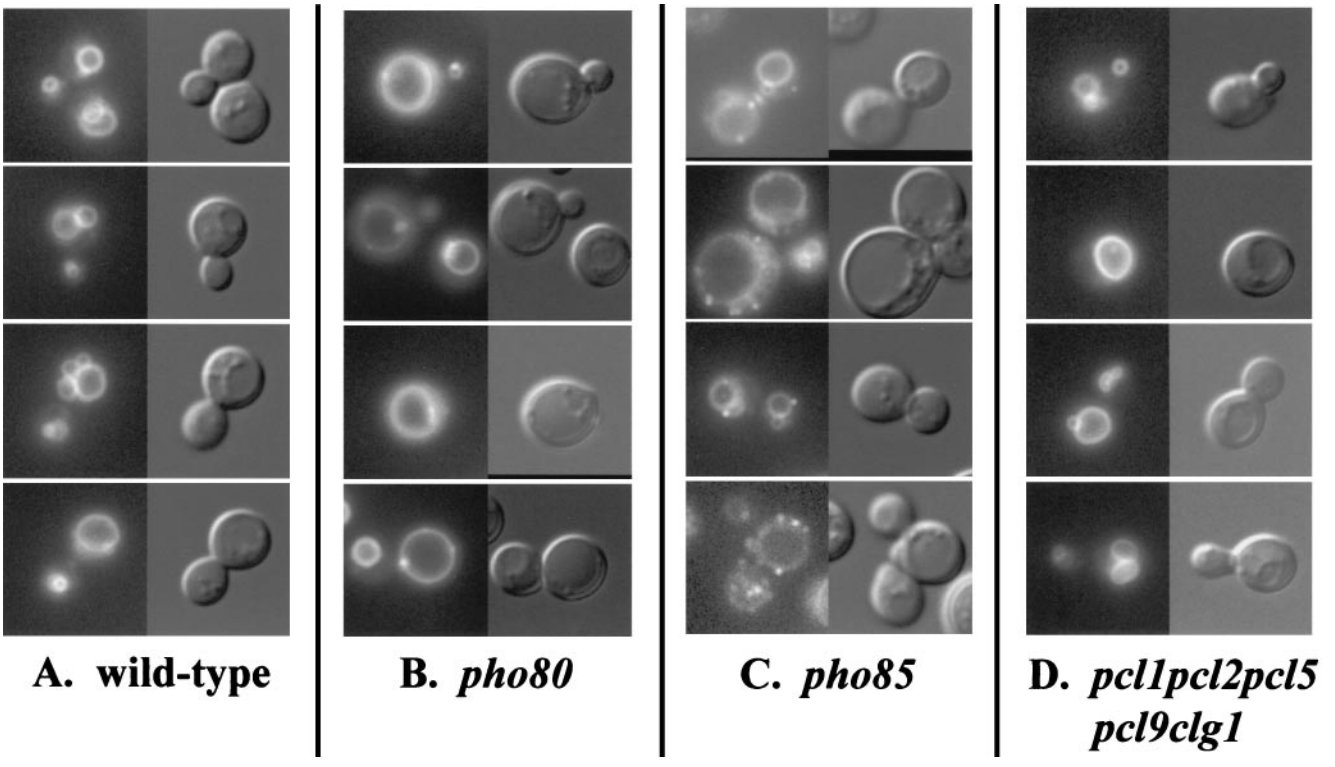

FIG. 5. Assay of membrane internalization and vacuolar membrane staining in wild-type, *pho85*Δ, *pho80*Δ, and quintuple-mutant strains. Bulk membrane internalization and transport to the vacuole were assayed by staining with the lipophilic styryl dye FM 4-64. (A) BY263 (wild type); (B) BY490 (*pho80*Δ); (C) BY391 (*pho85*Δ); (D) BY714 (*pcl1*Δ *pcl2*Δ *pcl5*Δ *pcl9*Δ *clg1*Δ). Cells were grown to mid-log phase (A_{600} = 0.4 to 0.6) and stained, and FM4-64 fluorescence was visualized with rhodamine fluorescence optics at a magnification of ×1,000 (see Materials and Methods).

we had uncovered a defect in vacuole function and morphology in *pho80* and *pho85* mutants (see above and Fig. 5).

VTC4 encodes a putative membrane-associated protein that is involved in vacuolar polyphosphate accumulation (9, 51). Interestingly, *VTC4*/*PHM3* is a Pho4-regulated gene and is thus highly expressed in *pho85*Δ and *pho80*Δ cells (Fig. 2A) (51). The sensitivity of *pho85*Δ cells to Ca^{2+} is solely dependent on the Pho80 cyclin (Fig. 3A and 5). Since the primary role of Pho80-Pho85 is to mediate the nuclear export of Pho4 and down-regulation of Pho4-dependent genes (30), we hypothesized that deletion of either *PHO4* or *VTC4* in a *pho80*Δ background should rescue the Ca^{2+} sensitivity of *pho80*Δ cells. Indeed, *pho80*Δ *pho4*Δ and *pho80*Δ *vtc4*Δ cells grew well on YPD plates supplemented with Ca^{2+} (Fig. 4; note that the *pho4*Δ strain was not recovered in our SGA suppressor screen since it is lost during the SGA screening process). Deletion of *PHO4* or *VTC4* in a *pho80*Δ background also rescued other Pho80-dependent *pho85*Δ phenotypes, including 4-NQO sensitivity and osmosensitivity (Fig. 4). These results suggest that *VTC4* is a key target of Pho4 and that Pho80-Pho85-mediated regulation of *VTC4* expression is crucial for yeast cell survival in variety of suboptimal conditions.

Electron microscopy reveals severe abnormalities in vacuole structure and function in *pho80* and *pho85* mutants dependent on the Pho4 target gene, *VTC4*. Our observations linking Pho80-Pho85 and *VTC4* to the cell stress response and vacuolar function prompted us to undertake an ultrastructural analysis of *pho85*Δ and *pho80*Δ cells. In wild-type cells, the majority of vacuoles were visible as electron-dense compartments that measured anywhere between 0.5 to 2 μm in diameter (Fig. 7A and B). Many wild-type cells with medium-sized buds had a characteristic vacuole streaming pattern from the mother into the bud (Fig. 7B) (6). Deletion of *PHO85* caused a dramatic phenotype with many misshapen cells and vacuoles that were almost exclusively transparent and extremely large, measuring between 2 to 8 μm in diameter with an average diameter of ~5 μm (Fig. 7C and D). The internal structure of the vacuoles in *pho85*Δ cells appeared largely disorganized, with one of the following characteristics: (i) small loop-like structures or mul-

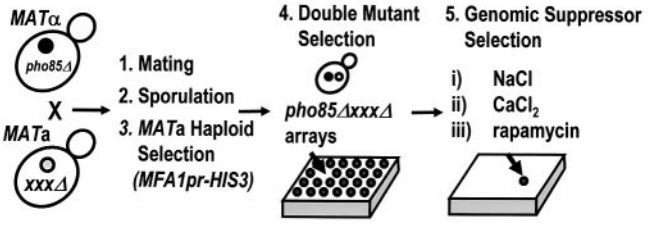

FIG. 6. SGA methodology for isolation of genomic suppressors. *pho85*Δ *xxx*Δ arrays were generated by (i) mating the query *MAT*α *pho85*Δ strain to an ordered array of *MAT***a** viable yeast deletion mutants, (ii) sporulation, (iii) haploid selection (64) by plating onto media lacking arginine and histidine with added canavanine, and (iv) double-mutant selection. The *pho85*Δ *xxx*Δ arrays were then printed onto plates containing 6% NaCl, 10 ng of rapamycin/ml, or 200 mM $CaCl_2$ for selection of genomic suppressors.

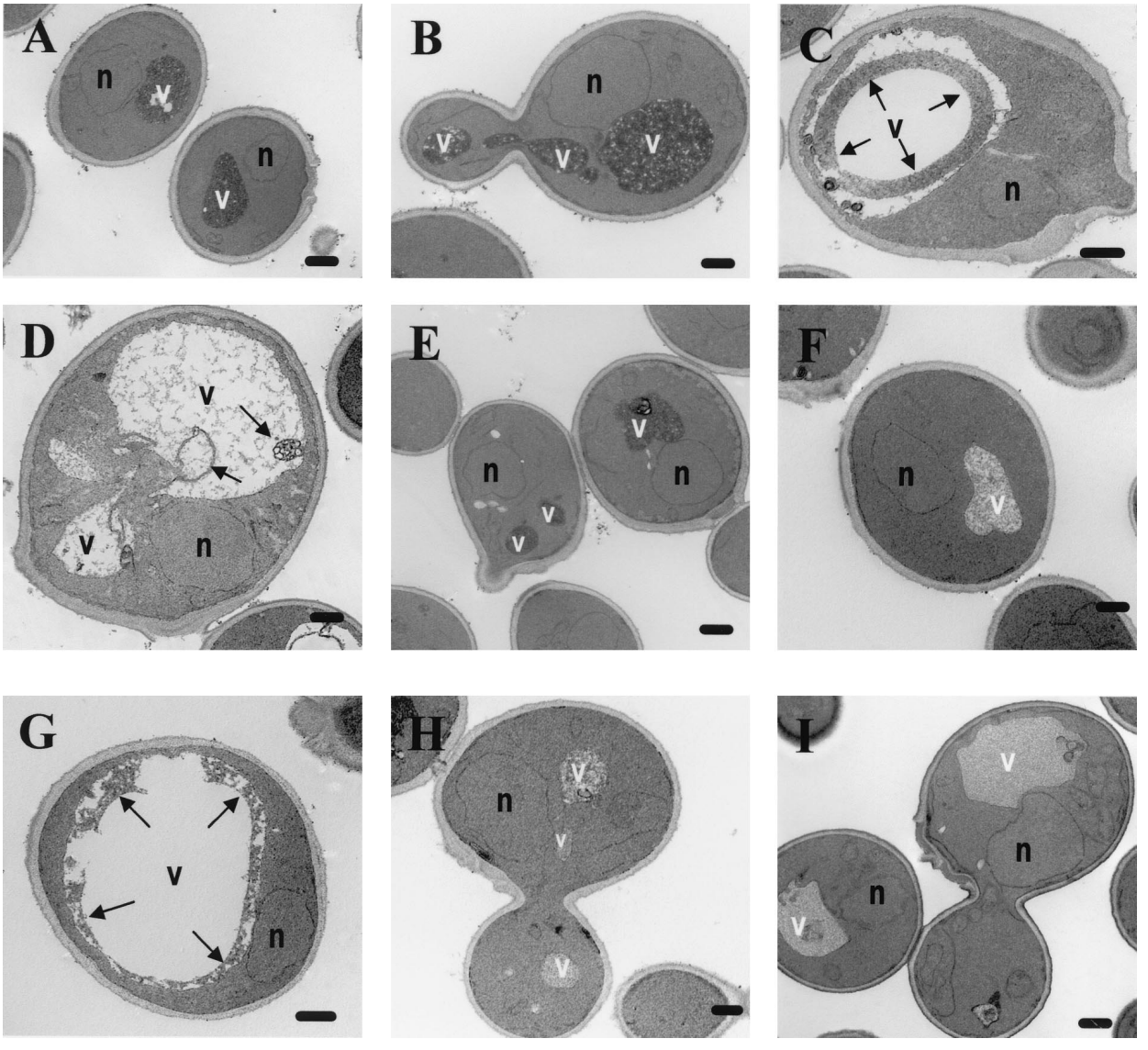

FIG. 7. Electron micrographs of cells lacking Pho80-Pho85, Pho4, and Vtc4. Cells were grown in rich medium (YPD) at 30°C to mid-log phase (A_{600} = 0.4) and prepared for electron microscopy as described in Materials and Methods. Examples of the following haploid cells are shown: wild type (A and B), *pho85*Δ cells (C and D), *pho85*Δ *pho4*Δ cells (E), *pho85*Δ *vtc4*Δ cells (F), *pho80*Δ cells (G), *pho80*Δ *pho4*Δ cells (H), *pho80*Δ *vtc4*Δ cells (I). Arrows in panels C and G indicate electron-dense structures that appear to be large circular vesicles or their predecessors in *pho85*Δ and *pho80*Δ cells. Arrows in panel D indicate smaller, multivesiculated vesicles within the vacuole of *pho85*Δ. n, nucleus; v, vacuole. Bars, 500 nm.

tivesiculated bodies (Fig. 7D), or (ii) a large spherical vesicle with a thick membrane (Fig. 7C). In many cases the intravacuolar structure appeared to be sloughing from the vacuolar membrane (Fig. 7G). The same vacuolar phenotype was seen in *pho80*Δ mutants except that the majority of the cells contained a single large vesicle within the vacuole that had either completely formed or was sloughing from the vacuolar membrane (Fig. 7G). Genetic evidence supports the idea that these internal vacuolar structures may represent some sort of autophagic vesicle (69). Consistent with our genetic suppression data, deletion of *PHO4* or *VTC4* in a *pho85*Δ or *pho80*Δ background largely corrected the vacuolar defects in these strains (Fig. 7E, F, H, and I). We conclude that *pho85*Δ and *pho80*Δ cells have abnormal vacuoles at the ultrastructural level and that these abnormalities are dependent on *PHO4* and its target gene *VTC4*.

To monitor the effects of *PHO4* and *VTC4* deletion on vacuole function in *pho85*Δ and *pho80*Δ cells, we used LY, which is actively transported into the yeast vacuole, as a nonspecific marker for endocytosis (67). Previous work showed that *pho85*Δ and quintuple-mutant (*pcl1 pcl2 pcl5 pcl9 clg1*) cells are defective in LY accumulation in the vacuole, but *pho80*Δ mutants were not tested (31). We found that *pho80*Δ mutants were impaired in their uptake of LY (Fig. 8). Again, deletion of *PHO4* or *VTC4* in a *pho80*Δ background restored the ability of *pho80*Δ cells to endocytose LY (Fig. 8), indicating that overexpression of *VTC4* is detrimental to vacuole-related processes. Our results suggest that transport of materials to the

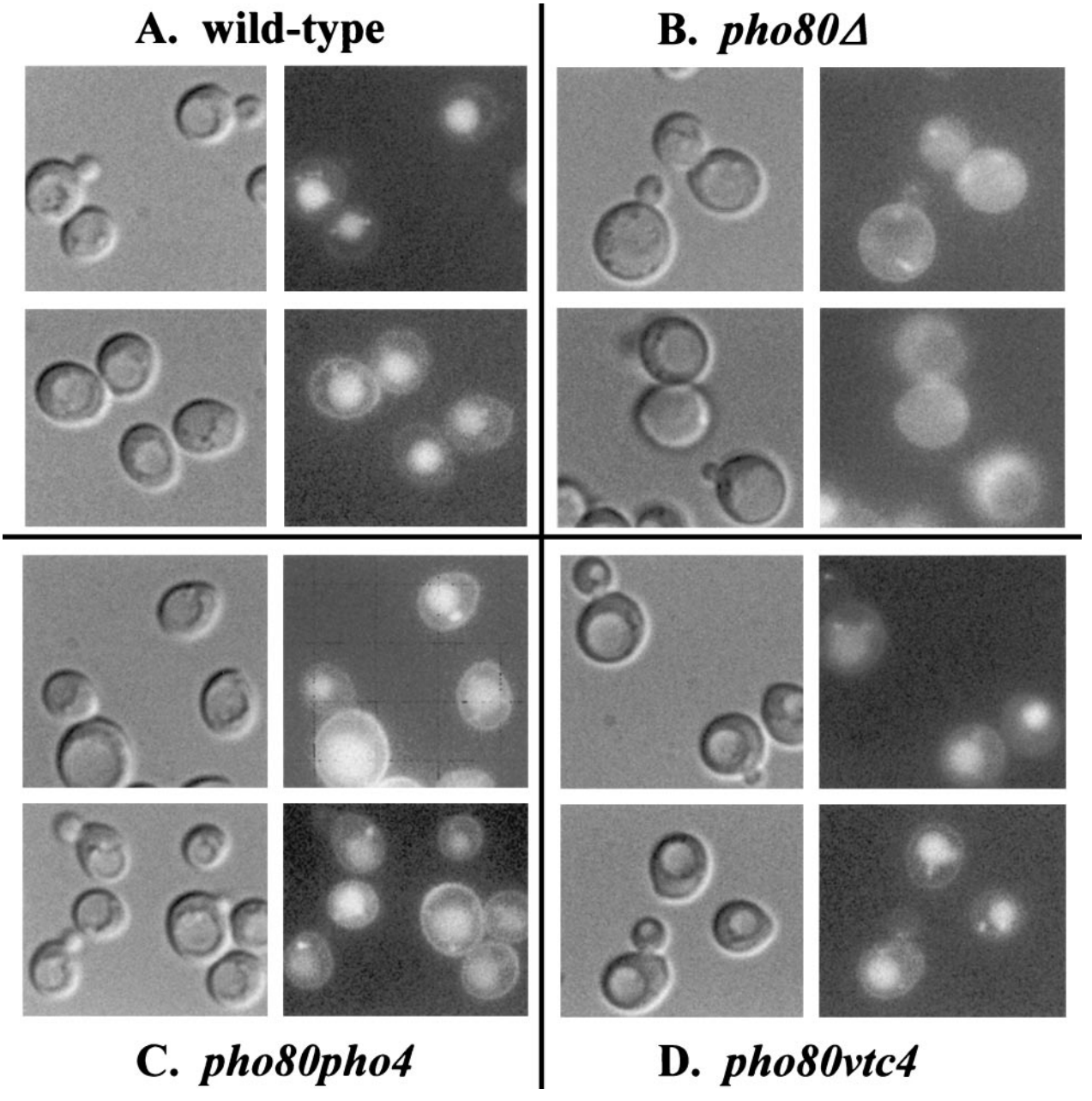

FIG. 8. Assay of endocytosis in wild-type, *pho85*, *pho80*Δ *pho4*Δ, and *pho80*Δ *vtc4*Δ cells. Fluid phase endocytosis was assayed by using LY on the following strains: BY263 (A), BY490 (B), BY1500 (C), and BY1501 (D). Cells were grown to mid-log phase and stained, and LY accumulation in the vacuole was visualized with fluorescein isothiocyanate fluorescence optics and photographed at a magnification of ×1,000 with an imaging system (see Materials and Methods).

vacuole is highly dependent on the Pho4 target gene *VTC4* and that Vtc4 plays an important role in vacuole function.

DISCUSSION

In this study, we used a functional-genomics approach to explore the biological basis of the complex phenotype caused by deletion of the multifunctional Pho85 Cdk. Pho85 function is mediated through 10 Pho85 cyclins or Pcls, but both the complexity of Pho85 function and the genetic redundancy of the cyclins have hampered efforts to use traditional genetic approaches to discover functions and substrates for individual Pcl-Pho85 complexes (45). Using a combination of SGA analysis (64), expression profiling, and phenotypic tests, we have uncovered important roles for Pho85 in cell integrity and the response to adverse growth conditions. First, our work highlights a cell integrity function for the Pcl1,2 subfamily of Pho85 Cdks that is independent of the role of Pho80-Pho85 in the response to stress. Second, we uncovered a key function for Pho80-Pho85-mediated regulation of Pho4 in vacuolar function and stress response, in addition to its well-established role in phosphate regulation. The integration of multiple genomics

approaches is likely to be a generally useful strategy for extracting functional information from pleiotropic mutant phenotypes.

An important component of our study was the application of a new genomics approach called SGA analysis; by this method, an array of viable haploid deletion mutants were screened for strains that were inviable in the absence of *PHO85* (64). The marked growth defect of *pho85* mutants led to a significant number of false positives in our initial pilot screens and required modification of the SGA method to accommodate mutant strains with a severe growth phenotype. The query strain, in our case the *pho85* mutant strain, is first transformed with a plasmid carrying the wild-type gene with a counter-selectable marker. In this way, the starting strain that is crossed to the yeast deletion array is essentially wild type; an array of double-mutant strains carrying the wild-type plasmid is recovered, and synthetic growth defects in the double mutants are only scored after selecting against the wild-type plasmid on the appropriate medium. We found that this simple modification to the SGA method significantly reduced the false-positive rate associated with our screen.

The advantage of SGA analysis over traditional synthetic-lethal screening procedures is that it is both speedy and relatively straightforward; we found that 53 genes are required for viability in a *pho85*Δ mutant using this procedure (Fig. 1). This profile of genetic interactions significantly expands the results of a previous conventional genetic screen and tests that have revealed 10 genetic interactions or *PHO85*-requiring genes (23, 33). *BEM2*, *BCK1*, *CLA4*, and *SLT2*/*MPK1* were identified by both methods. Both *EFR3* and *GCR1* were identified as *PHO85*-requiring genes (33), but mutants lacking *EFR3* or *GCR1* were not represented on our original array of deletion mutants. Also, three strains with deletions of other *PHO85*-requiring genes, *SPT7*, *SRB5*, or *HFI*, were unrecoverable by our modified screening procedure (see Materials and Methods). Therefore, our SGA screen obtained four out of seven possible genes known to be required in the absence of *PHO85*. Direct genetic tests also revealed a genetic interaction of *PHO85* with the essential GTPase gene *CDC42*, which cannot be scored by our present array of haploid viable deletion mutants. Systematic construction of arrays of strains harboring conditional alleles of essential genes will allow the over 1,000 genes that are required for haploid viability (71) to be queried by using SGA methodology. Despite the present limitations of our screen, we uncovered over 40 new Pho85-requiring genes, the vast majority of which point to a significant role for Pho85 in cell integrity.

Because obvious functional groups of genes were captured in our systematic *pho85*Δ synthetic-lethal screen, we used DNA microarrays to ask if *pho85*Δ or *pcl*Δ transcriptional profiles had a detectable signature that correlated with the *pho85*Δ genetic profile. In a previous study, Ogawa et al. explored the global transcriptional consequence of constitutive activation of the phosphate response system in budding yeast by deleting either component of the Pho80-Pho85 Cdk (51). In the absence of Pho80-Pho85, the Pho4 transcription factor is largely nuclear and promotes constitutive activation of phosphate-responsive genes including *PHO5*, an acid phosphatase gene (see references 28 and 30 for reviews). In addition to the canonical *PHO* cluster of genes, Ogawa et al. identified several other phosphate-responsive genes that are targets of Pho4 (51); some of the so-called *PHM* genes are involved in polyphosphate synthesis, and some were previously identified as *VTC* genes involved in vacuolar function (9). A second microarray analysis used chemical inhibition of an analogue-sensitive allele of the Pho85 gene to explore the immediate consequences of depletion of Pho85. The entire *PHO* cluster, including most of the *PHM* genes as well as genes involved in reserve carbohydrate metabolism, were affected by depletion of *PHO85* (5). Our data set correlates significantly with both of these microarray studies when the 546 representative genes used in the analysis shown in Fig. 2 are used (ρ, ~0.3). However, neither of these microarray studies uncovered any evidence that *PHO85* was required for cell integrity or polarized growth. In our study, we compared the expression signatures of *pho85*Δ and *pcl*Δ mutant strains to each other and also to a diverse set of reference profiles (24). No single *pcl*Δ mutant strain or combination of *pcl*Δ mutations in a single strain had an expression profile that correlated well to that of the *pho85*Δ strain over all available genes (data not shown). However, the expression profile of a *pho85*Δ mutant had a significant degree of similarity to mutants with cell integrity or ergosterol defects (Fig. 2). Our results highlight the importance of comparing expression signatures in a DNA microarray analysis of mutant strains with complex phenotypes and corroborate our SGA results pointing to a cell integrity function for Pho85.

In an effort to discover the cyclins that contribute to the cell integrity function in *pho85* mutants, we tested the sensitivity of *pho85*Δ and *pcl* mutants to a variety of structurally and functionally distinct compounds. These phenotypic tests revealed at least two defects that contribute to the widespread sensitivity of *pho85*Δ mutants to cellular insults. First, *pho85* mutants are highly sensitive to reagents or conditions that damage the cell wall, and this phenotype is largely attributable to the Pcl1,2 subfamily of cyclins. We have tested directly for alterations in ergosterol, lipids, and phospholipids in *pho85* mutants and have found no obvious defect in cell membrane composition. We infer that Pho85 is unlikely to play a direct role in cell wall or membrane construction or maintenance. Rather, this study and a number of other observations strongly suggest that the Pcl1,2-type Pho85 Cdks ensure cell integrity through regulation of cell polarity and the actin cytoskeleton. As summarized in the introduction, expression of *PCL1*, *PCL2*, and *PCL9*, which encode three members of the Pcl1,2 subfamily, is entirely restricted to the G_1 phase of the cell cycle, and our previous work has identified an actin cytoskeletal protein, Rvs167, as a strong candidate substrate for Pcl1,2-Pho85 Cdks. This study and other genetic data clearly show that additional targets of the Pcl1,2-type Pho85 Cdks related to their role in cell morphogenesis and polarity remain to be discovered (44, 45). Although our functional-genomics approaches failed to identify new cell integrity targets of Pho85 Cdks, our screens strongly support the view that Pho85 is essential for elaboration of the bud and cell cycle progression when other cell polarity regulators are chemically or genetically compromised (2, 39, 40).

Our efforts to dissect the complex cell integrity phenotypes of *pho85* mutants also revealed a second major defect that accounts for the sensitivity of the *pho85* strain to a spectrum of compounds and genetic alterations. We used a modification of

the SGA method to screen for genomic suppressors of stress sensitivities seen in the *pho85* mutant. This rapid screening method allowed us to attribute aspects of the *pho85* phenotype to specific downstream targets of Pho85; we found that the sensitivity of both *pho80* and *pho85* mutants to a variety of stresses is dependent on the Pho4-regulated gene *VTC4*. Using electron microscopy and genetic suppression, we found that *pho85* and *pho80* mutants have marked defects in vacuole structure and function that can be bypassed by deletion of either *PHO4* or *VTC4*. We conclude that the stress sensitivities of *pho85*Δ mutants can be largely explained by major defects in vacuole structure and function due to inappropriate expression of *VTC4*. Further, our results strongly suggest that phosphorylation of Pho4 by Pho80-Pho85 regulates the response not only to extracellular phosphate levels but also to other environmental stresses (pH, carbon source, ions, and osmolarity).

The application of systematic and rapid functional-genomics approaches has allowed us to attribute many of the stress sensitivities of *pho85*Δ mutants to misregulation of *VTC4* and has highlighted the highly deleterious effect of misregulation of Pho4. An analysis of the biochemical function of Vtc4 is required to determine the precise biological basis of the vacuolar phenotype in cells lacking the Pho80-Pho85 Cdk. The dramatic effects on cell ultrastructure caused by unrestrained Pho4 activity may well obscure the cell integrity and polarity functions of other Pho85 Cdks; our results predict that further genetic and biochemical analysis of the cell integrity defect in a *pho85 vtc4* double mutant will enlighten us about the independent role for Pcl1,2-type Pho85 kinases in cell integrity.

ACKNOWLEDGMENTS

We are grateful to Alan Davidson, Helena Friesen, and Bri Lavoie for discussion and comments on the manuscript. We thank Martin Bard (Purdue University) for analysis of sterol composition in *pho85* mutant strains and Cliff Lingwood (Hospital for Sick Children, Toronto) for expert advice.

D.H. was a postdoctoral fellow of the National Cancer Institute of Canada and was supported by funds provided by the Terry Fox Run. J.M. held a Doctoral Award from the Canadian Institutes of Health Research (CIHR), and B.A. is a CIHR Scientist. This work was supported by an operating grant from the National Cancer Institute of Canada with funds from the Canadian Cancer Society. Our SGA laboratories are supported by a Collaborative Genomics Special Project grant from the Canadian Institutes of Health Research and by funds from Genome Canada through the Ontario Genomics Institute.

D. Huang and J. Moffat contributed equally to this work.

REFERENCES

1. **Aerne, B. L., A. L. Johnson, J. Toyn, and L. Johnston.** 1998. Swi5 controls a novel wave of cyclin synthesis in late mitosis. Mol. Biol. Cell **9:**945–956.
2. **Andrews, B., and V. Measday.** 1998. The cyclin family of budding yeast: abundant use of a good idea. Trends Genet. **14:**66–72.
3. **Baetz, K., J. Moffat, J. Haynes, M. Chang, and B. Andrews.** 2001. Transcriptional coregulation by the cell integrity mitogen-activated protein kinase Slt2 and the cell cycle regulator Swi4. Mol. Cell. Biol. **21:**6515–6528.
4. **Botstein, D., D. Amberg, J. Mulholland, T. Huffaker, A. Adams, D. Drubin, and T. Stearns.** 1997. The yeast cytoskeleton, p. 1–90. *In* J. Pringle, J. Broach, and E. Jones (ed.), The molecular and cellular biology of the yeast *Saccharomyces*, vol. 3. Cold Spring Harbor Laboratory Press, Cold Spring Harbor, N.Y.
5. **Carroll, A. S., A. C. Bishop, J. L. DeRisi, K. M. Shokat, and E. K. O'Shea.** 2001. Chemical inhibition of the Pho85 cyclin-dependent kinase reveals a role in the environmental stress response. Proc. Natl. Acad. Sci. USA **98:** 12578–12583.
6. **Catlett, N. L., and L. S. Weisman.** 2000. Divide and multiply: organelle partitioning in yeast. Curr. Opin. Cell Biol. **12:**509–516.
7. **Chan, T.-F., J. Carvalho, L. Riles, and X. F. S. Zheng.** 2000. A chemical genomics approach toward understanding the global functions of the target of rapamycin protein (TOR). Proc. Natl. Acad. Sci. USA **97:**13227–13232.
8. **Chi, Y., M. J. Huddleston, X. Zhang, R. A. Young, R. S. Annan, S. A. Carr, and R. Deshaies.** 2001. Negative regulation of Gcn4 and Msn2 transcription factors by Srb10 cyclin-dependent kinase. Genes Dev. **15:**1078–1092.
9. **Cohen, A., N. Perzov, H. Nelson, and N. Nelson.** 1999. A novel family of yeast chaperones involved in the distribution of V-ATPase and other membrane proteins. J. Biol. Chem. **274:**26885–26893.
10. **Colwill, K., D. Field, L. Moore, J. Friesen, and B. Andrews.** 1999. *In vivo* analysis of the domains of yeast Rvs167p suggests Rvs167p function is mediated through multiple protein interactions. Genetics **152:**881–893.
11. **Delley, P. A., and M. N. Hall.** 1999. Cell wall stress depolarized cell growth via hyperactivation of RHO1. J. Cell Biol. **147:**163–174.
12. **Dhavan, R., and L.-H. Tsai.** 2001. A decade of CDK5. Nat. Rev. Mol. Cell Biol. **2:**749–759.
13. **Drees, B. L., B. Sundin, E. Brazeau, J. P. Caviston, G. C. Chen, W. Guo, K. G. Kozminski, M. W. Lau, J. J. Moskow, A. Tong, L. R. Schenkman, A. McKenzie, P. Brennwald, M. Longtine, E. Bi, C. Chan, P. Novick, C. Boone, J. R. Pringle, T. N. Davis, S. Fields, and D. G. Drubin.** 2001. A protein interaction map for cell polarity development. J. Cell Biol. **154:**549–571.
14. **Espinoza, F. H., J. Ogas, I. Herskowitz, and D. O. Morgan.** 1994. Cell cycle control by a complex of the cyclin HCS26(PCL1) and the kinase PHO85. Science **266:**1388–1391.
15. **Forgac, M.** 2000. Structure, mechanism and regulation of the clathrin-coated vesicle and yeast vacuolar H+-ATPases. J. Exp. Biol. **203:**71–80.
16. **Friesen, H., R. Lunz, S. Doyle, and J. Segall.** 1994. Mutation of the SPS1-encoded protein kinase of Saccharomyces cerevisiae leads to defects in transcription and morphology during spore formation. Genes Dev. **8:**2162–2175.
17. **Ghannoum, M. A., and L. B. Rice.** 1999. Antifungal agents: mode of action, mechanisms of resistance, and correlation of these mechanisms with bacterial resistance. Clin. Microbiol. Rev. **12:**501–517.
18. **Graham, L. A., B. Powell, and T. H. Stevens.** 2000. Composition and assembly of the yeast vacuolar H+-ATPase complex. J. Exp. Biol. **203:**61–70.
19. **Gustin, M. C., J. Albertyn, M. Alexander, and K. Davenport.** 1998. MAP kinase pathways in the yeast *Saccharomyces cerevisiae*. Microbiol. Mol. Biol. Rev. **62:**1264–1300.
20. **Guthrie, C., and G. R. Fink.** 1991. Guide to yeast genetics and molecular biology. Methods Enzymol. **194:**3–302.
21. **Hardwick, K. G., M. J. Lewis, J. Semenza, N. Dean, and H. R. Pelham.** 1990. ERD1, a yeast gene required for the retention of luminal endoplasmic reticulum proteins, affects glycoprotein processing in the Golgi apparatus. EMBO J. **9:**623–630.
22. **Huang, D., J. Moffat, W. A. Wilson, L. Moore, P. J. Roach, and B. J. Andrews.** 1998. Cyclin partners determine Pho85 protein kinase substrate specificity in vitro and in vivo: control of glycogen biosynthesis by Pcl8 and Pcl10. Mol. Cell. Biol. **18:**3289–3299.
23. **Huang, D., G. Patrick, J. Moffatt, L.-H. Tsai, and B. Andrews.** 1999. Mammalian Cdk5 is a functional homologue of the budding yeast Pho85 cyclin-dependent protein kinase. Proc. Natl. Acad. Sci. USA **96:**14445–14450.
24. **Hughes, T. R., M. J. Marton, A. R. Jones, C. J. Roberts, R. Stoughton, C. D. Armour, H. A. Bennett, E. Coffey, H. Dai, Y. He, M. J. Kidd, A. King, M. Meyer, D. Slade, P. Lum, S. Stepaniants, D. Shoemaker, D. Gachotte, K. Chakrabortty, J. Simon, M. Bard, and S. Friend.** 2000. Functional discovery via a compendium of expression profiles. Cell **102:**109–126.
25. **Johnson, D. I.** 1999. Cdc42: an essential Rho-type GTPase controlling eukaryotic cell polarity. Microbiol. Mol. Biol. Rev. **63:**54–105.
26. **Jungmann, J., and S. Munro.** 1998. Multi-protein complexes in the cis Golgi of Saccharomyces cerevisiae with alpha-1,6-mannosyltransferase activity. EMBO J. **17:**423–434.
27. **Kaffman, A., I. Herskowitz, R. Tjian, and E. O'Shea.** 1994. Phosphorylation of the transcription factor Pho4 by a cyclin-cdk complex, Pho80-Pho85. Science **263:**1153–1158.
28. **Kaffman, A., and E. K. O'Shea.** 1999. Regulation of nuclear localization: a key to a door. Annu. Rev. Cell Dev. Biol. **15:**291–339.
29. **Kane, P. M., and K. J. Parra.** 2000. Assembly and regulation of the yeast vacuolar H+-ATPase. J. Exp. Biol. **203:**81–87.
30. **Komeili, A., and E. K. O'Shea.** 2001. New perspectives on nuclear transport. Annu. Rev. Genet. **35:**341–364.
31. **Lee, J., K. Colwill, V. Aneliunas, C. Tennyson, L. Moore, Y. Ho, and B. Andrews.** 1998. Interaction of yeast Rvs167 and Pho85 cyclin-dependent kinase complexes may link the cell cycle to the actin cytoskeleton. Curr. Biol. **8:**1310–1321.
32. **Lee, M., S. O'Regan, J.-L. Moreau, A. L. Johnson, L. H. Johnston, and C. R. Goding.** 2000. Regulation of the Pcl7-Pho85 cyclin-cdk complex by Pho81. Mol. Microbiol. **38:**411–422.
33. **Lenburg, M. E., and E. K. O'Shea.** 2001. Genetic evidence for a morphogenetic function of the *Saccharomyces cerevisiae* Pho85 cyclin-dependent kinase. Genetics **157:**39–51.
34. **Lenburg, M. E., and E. K. O'Shea.** 1996. Signaling phosphate starvation. Trends Biochem. Sci. **21:**383–387.
35. **Longtine, M. S., A. McKenzie, D. J. Demarini, N. G. Shah, A. Wach, A.**

Brachat, P. Philippsen, and J. R. Pringle. 1998. Additional modules for versatile and economical PCR-based gene deletion and modification in Saccharomyces cerevisiae. Yeast **14:**953–961.
36. **Madden, K., Y.-J. Sheu, K. Baetz, B. Andrews, and M. Snyder.** 1997. SBF cell cycle regulator as a target of the yeast PKC-MAP kinase pathway. Science **275:**1781–1784.
37. **McBride, H. J., A. Sil, V. Measday, Y. Yu, J. Moffat, M. E. Maxon, I. Herskowitz, B. Andrews, and D. J. Stillman.** 2001. The protein kinase Pho85 is required for asymmetric accumulation of the Ash1 protein in *Saccharomyces cerevisiae*. Mol. Microbiol. **42:**345–353.
38. **Measday, V., H. McBride, J. Moffat, D. Stillman, and B. Andrews.** 2000. Interactions between Pho85 cyclin-dependent kinase complexes and the Swi5 transcription factor in budding yeast. Mol. Microbiol. **35:**825–834.
39. **Measday, V., L. Moore, J. Ogas, M. Tyers, and B. Andrews.** 1994. The PCL2 (ORFD)-PHO85 cyclin-dependent kinase complex: a cell cycle regulator in yeast. Science **266:**1391–1395.
40. **Measday, V., L. Moore, R. Retnakaran, J. Lee, M. Donoviel, A. M. Neiman, and B. Andrews.** 1997. A family of cyclin-like proteins that interact with the Pho85 cyclin-dependent kinase, Pho85. Mol. Cell. Biol. **17:**1212–1223.
41. **Meiomoun, A., T. Holtzman, Z. Weissman, H. McBride, D. J. Stillman, G. R. Fink, and D. Kornitzer.** 2000. Degradation of the transcription factor Gcn4 requires the kinase Pho85 and the SCFcdc4 ubiquitin-ligase complex. Mol. Biol. Cell **11:**915–927.
42. **Mendenhall, M. D., and A. E. Hodge.** 1998. Regulation of Cdc28 cyclin-dependent protein kinase activity during the cell cycle of the yeast *Saccharomyces cerevisiae*. Microbiol. Mol. Biol. Rev. **62:**1191–1243.
43. **Miller, M. E., and F. R. Cross.** 2001. Cyclin specificity: how many wheels do you need on a unicycle? J. Cell Sci. **114:**1811–1820.
44. **Miller, M. E., and F. R. Cross.** 2001. Mechanisms controlling subcellular localization of the G_1 cyclins Cln2p and Cln3p in budding yeast. Mol. Cell. Biol. **21:**6292–6311.
45. **Moffat, J., D. Huang, and B. J. Andrews.** 2000. Functions of Pho85 cyclin-dependent kinases in budding yeast. Prog. Cell Cycle Res. **4:**97–106.
46. **Morgan, D. O.** 1997. Cyclin-dependent kinases: engines, clocks and microprocessors. Annu. Rev. Cell Dev. Biol. **13:**261–291.
47. **Nicolson, T., B. Conradt, and W. Wickner.** 1996. A truncated form of the Pho80 cyclin of *Saccharomyces cerevisiae* induces expression of a small cytosolic factor which inhibits vacuole inheritance. J. Bacteriol. **178:**4047–4051.
48. **Nicolson, T. A., L. S. Weisman, G. S. Payne, and W. T. Wickner.** 1995. A truncated form of the Pho80 cyclin redirects the Pho85 kinase to disrupt vacuole inheritance in *S. cerevisiae*. J. Cell Biol. **130:**835–845.
49. **Nishizawa, M., M. Kawasumi, M. Fujino, and A. Toh-e.** 1998. Phosphorylation of Sic1, a cyclin-dependent kinase (Cdk) inhibitor, by Cdk including Pho85 kinase is required for its prompt degradation. Mol. Biol. Cell **9:**2393–2405.
50. **Nishizawa, N., Y. Kanaya, and A. Toh-e.** 1999. Mouse cyclin-dependent kinase (Cdk)5 is a functional homologue of a yeast Cdk, Pho85 kinase. J. Biol. Chem. **274:**33859–33862.
51. **Ogawa, N., J. DeRisi, and P. O. Brown.** 2000. New components of a system for phosphate accumulation and polyphosphate metabolism in *Saccharomyces cerevisiae* revealed by genomic expression analysis. Mol. Biol. Cell **11:**4309–4321.
52. **O'Neill, E. M., A. Kaffman, E. R. Jolly, and E. K. O'Shea.** 1996. Regulation of Pho4 nuclear localization by the Pho80-Pho85 cyclin-CDK complex. Science **271:**209–212.
53. **Ovalle, R., S. T. Lim, B. Holder, C. K. Jue, C. W. Moore, and P. N. Lipke.** 1998. A spheroplast rate assay for determination of cell wall integrity in yeast. Yeast **14:**1159–1166.
54. **Parks, L. W., S. J. Smith, and J. H. Crowley.** 1995. Biochemical and physiological effects of sterol alterations in yeast. Lipids **30:**227–230.
55. **Popova, I. G., M. V. Padkina, and E. V. Sambuk.** 2000. Effect of mutations in PHO85 and PHO4 genes on utilization of proline in Saccharomyces cerevisiae yeasts. Genetika **36:**1622–1628.
56. **Pruyne, D., and A. Bretscher.** 2000. Polarization of cell growth in yeast. II. The role of the cortical actin cytoskeleton. J. Cell Sci. **113:**571–585.
57. **Rine, J., W. Hansen, E. Hardeman, and R. W. Davis.** 1983. Targeted selection of recombinant clones through gene dosage effects. Proc. Natl. Acad. Sci. USA **80:**6750–6754.
58. **Rudolph, H. K., A. Antebi, G. R. Fink, C. M. Buckley, T. E. Dorman, J. LeVitre, L. S. Davidow, J. I. Mao, and D. T. Moir.** 1989. The yeast secretory pathway is perturbed by mutations in PMR1, a member of a Ca2+ ATPase family. Cell **58:**133–145.
59. **Schneider, K. R., R. L. Smith, and E. K. O'Shea.** 1994. Phosphate-regulated inactivation of the kinase Pho80-Pho85 by the CDK inhibitor Pho81. Science **266:**122–126.
60. **Shahinian, S., and H. Bussey.** 2000. β-1,6-Glucan synthesis in Saccharomyces cerevisiae. Mol. Microbiol. **35:**477–489.
61. **Tennyson, C., J. Lee, and B. Andrews.** 1998. A role for the Pcl9-Pho85 cyclin-Cdk complex at the M/G1 boundary in *Saccharomyces cerevisiae*. Mol. Microbiol. **28:**69–79.
62. **Thevelein, J. M., and J. H. de Winde.** 1999. Novel sensing mechanisms and targets for the cAMP-protein kinase A pathway in the yeast *Saccharomyces cerevisiae*. Mol. Microbiol. **33:**904–918.
63. **Timblin, B. K., K. Tatchell, and L. Bergman.** 1996. Deletion of the gene encoding the cyclin-dependent protein kinase Pho85 alters glycogen metabolism in *Saccharomyces cerevisiae*. Genetics **143:**57–66.
64. **Tong, A. H. Y., M. Evangelista, A. B. Parsons, H. Xu, G. D. Bader, N. Page, M. Robinson, S. Raghibizadeh, C. W. V. Hogue, H. Bussey, B. Andrews, M. Tyers, and C. Boone.** 2001. Systematic genetic analysis with ordered arrays of yeast deletion mutants. Science **294:**2364–2368.
65. **Tyers, M., and P. Jorgensen.** 2000. The cell cycle, p. 58–105. *In* P. Fantes and J. Beggs (ed.), The yeast nucleus: frontiers in molecular biology. Oxford University Press, Oxford, United Kingdom.
66. **Verna, J., A. Lodder, K. Lee, A. Vagts, and R. Ballester.** 1997. A family of genes required for maintenance of cell wall integrity and for the stress response in Saccharomyces cerevisiae. Proc. Natl. Acad. Sci. USA **94:**13804–13809.
67. **Vida, T. A., and S. D. Emr.** 1995. A new vital stain for visualizing vacuolar membrane dynamics and endocytosis in yeast. J. Cell Biol. **128:**779–792.
68. **Wang, Z., W. Wilson, M. Fujino, and P. J. Roach.** 2001. The yeast cyclins Pcl6p and Pcl7p are involved in the control of glycogen storage by the cyclin-dependent protein kinase Pho85p. FEBS Lett. **506:**277–280.
69. **Wang, Z., W. A. Wilson, M. A. Fujino, and P. J. Roach.** 2001. Antagonistic controls of autophagy and glycogen accumulation by Snf1p, the yeast homolog of AMP-activated protein kinase, and the cyclin-dependent kinase Pho85p. Mol. Cell. Biol. **21:**5742–5752.
70. **Wilson, W., A. M. Mahrenholz, and P. J. Roach.** 1999. Substrate targeting of the yeast cyclin-dependent kinase Pho85p by the cyclin Pcl10p. Mol. Cell. Biol. **19:**7020–7030.
71. **Winzeler, E. A., D. D. Shoemaker, A. Astromoff, H. Liang, K. Anderson, B. Andre, R. Bangham, R. Benito, J. D. Boeke, H. Bussey, A. M. Chu, C. Connelly, K. Davis, F. Dietrich, S. W. Dow, M. E. Bakkoury, F. Foury, S. H. Friend, E. Gentalen, G. Giaever, J. H. Hegemann, T. Jones, M. Laub, H. Liao, N. Liebundguth, D. J. Lockhart, and R. W. Davis.** 1999. Functional characterization of the *S. cerevisiae* genome by gene deletion and parallel analysis. Science **285:**901–906.